Bio-Design and Manufacturing (2018) 1:215–224
https://doi.org/10.1007/s42242-018-0028-8

REVIEW

Three-dimensional bioprinting of gelatin methacryloyl (GelMA)

Guoliang Ying[1,2] · Nan Jiang[3] · Cunjiang Yu[4] · Yu Shrike Zhang[1]

Received: 20 October 2018 / Accepted: 3 November 2018 / Published online: 16 November 2018

Abstract

The three-dimensional (3D) bioprinting technology has progressed tremendously over the past decade. By controlling the size, shape, and architecture of the bioprinted constructs, 3D bioprinting allows for the fabrication of tissue/organ-like constructs with strong structural–functional similarity with their in vivo counterparts at high fidelity. The bioink, a blend of biomaterials and living cells possessing both high biocompatibility and printability, is a critical component of bioprinting. In particular, gelatin methacryloyl (GelMA) has shown its potential as a viable bioink material due to its suitable biocompatibility and readily tunable physicochemical properties. Current GelMA-based bioinks and relevant bioprinting strategies for GelMA bioprinting are briefly reviewed.

Keywords Bioprinting · Bioink · Gelatin methacryloyl (GelMA) · Biofabrication · Tissue engineering · Tissue model

Introduction

The demand for organ replacement or tissue regeneration is quickly expanding, while the number of donor organs is far from sufficient [1, 2]. Tissue engineering, initially proposed approximately three decades ago, has thus emerged as an alternative strategy aiming to generate tissues and organs that are functionally relevant to their in vivo counterparts, to replace those that are damaged or diseased in the body [3]. Besides this conventional aspect, tissue engineering has found additional applications over the past years in serving as a tool to produce biomimetic miniaturized human tissue models for the purpose of improving the accuracy of drug screening and of promoting personalized medicine [4, 5]. Nevertheless, it is still a great challenge to fabricate complex living tissues except for a few simple organs such as skin [6] and cartilage [7]. Recently, the advancements in three-dimensional (3D) bioprinting seem to have brought us a step closer to realizing the ambitious aim of tissue engineering, by providing an unprecedented means to control, in precision, the deposition/patterning of cells and biomaterials in the volumetric space at high reproducibility [8].

While there are several bioprinting modalities commonly used for tissue fabrication, the bioink consisting of a mixture of biomaterial(s) and cell(s) is the unanimously vital component serving as the building block of bioprinted 3D tissue structures [9, 10]. Taking extrusion bioprinting as an example, the bioinks play key roles in dispersing the cells prior to bioprinting, in maintaining the integrity of the structures during bioprinting, and in supporting the adhesion, spreading, and functionality of encapsulated cells post-bioprinting [11, 12]. The bioprinted cell-laden constructs featuring arbitrary shapes and architectures finally form 3D tissue-like structures following a period of culture [13].

In principle, an ideal bioink should possess physicochemical properties suitable for the bioprinting process, and the bioprinted constructs should have proper biological and mechanical properties close to those of the native

Guoliang Ying and Nan Jiang have contributed equally to this work.

✉ Cunjiang Yu
cyu13@central.uh.edu

✉ Yu Shrike Zhang
yszhang@research.bwh.harvard.edu

1 Division of Engineering in Medicine, Department of Medicine, Brigham and Women's Hospital, Harvard Medical School, Cambridge, MA 02139, USA

2 School of Materials Science and Engineering, Wuhan Institute of Technology, Wuhan 430205, People's Republic of China

3 School of Engineering and Applied Sciences, Harvard University, Cambridge, MA 02139, USA

4 Departments of Mechanical Engineering, Electrical and Computer Engineering, Biomedical Engineering, Materials Science and Engineering Program, The Texas Center for Superconductivity, University of Houston, Houston, TX 77204, USA

tissues. Hydrogel-based bioinks encapsulating living cells and bioactive components are of particular interest for bioprinting [14]. To this end, numerous hydrogel-based bioink formulations such as gelatin methacryloyl (GelMA) [15–17], acrylate-functionalized poly(ethylene glycol) [18, 19], alginate [20, 21], agarose [22], and collagen [23] have been adopted, either used alone or in combinations, as bioinks. Among the different types of hydrogel bioinks, those based on GelMA hold good promise attributed to the superior biocompatibility, on-demand photocrosslinkability, and broadly tunable physicochemical properties of this biomacromolecule denatured from collagen [22]. This review outlines recent advances in the development of GelMA-based bioink formulations and strategies suitable for GelMA bioprinting.

GelMA-based bioink formulations

Pure GelMA bioink

To produce hydrogel constructs through extrusion bioprinting, it is necessary to control the viscosity of the bioink as an important rheological parameter [24]. High viscosity of the bioink is essential to maintain the structural fidelity of the extruded filaments deposited layer by layer in 3D. Direct bioprinting of pure GelMA hydrogel as the bioink has been a challenge because of its generally low viscosity at room or higher temperatures. Yet, GelMA could still be directly bioprinted through adjusting several parameters to reach appropriate viscosity: the concentration of the polymer, the temperature, and the degree of crosslinking [25]. First, higher viscosity can be obtained by increasing the concentration of the GelMA solution potentially allowing for high-fidelity bioprinting. The challenge associated with this approach is that the elevated concentration of GelMA solution (such as > 30 w/v%) will inevitably lead to low cell bioactivity due to the presence of the dense polymer network [26]. Second, owing to its temperature sensitiveness, reduced temperature at close to 0 °C would induce the formation of the GelMA physical gels (GPGs) that are shear-thinning and self-healing, enabling direct extrusion bioprinting of pure GelMA constructs at relatively low concentrations of the bioinks (down to 3 w/v%, Fig. 1A) [15, 17]. The formation of the GPGs could be achieved by cooling down the GelMA bioinks prior to bioprinting [15] or by using a cooling printhead during bioprinting [27–29]. In the third option, by taking advantage of the in situ crosslinking strategy, GelMA bioinks could be partially photocrosslinked during extrusion to enhance the viscosity and thus the fidelity of their direct extrusion bioprinting (Fig. 1B) [30].

Pore-forming GelMA bioink

Direct bioprinting of pure GelMA bioinks provides programmable and customizable platforms to engineer cell-laden constructs mimicking human tissues for a wide range of biomedical applications. However, the encapsulated cells are often restricted in spreading and proliferation by the relatively dense GelMA networks from gelation of the GelMA molecules at medium-to-high concentrations. A pore-forming GelMA-based bioink formulation was recently developed (Fig. 2A) to possibly overcome the aforementioned drawback of the conventional pure GelMA bioinks [31]. Such a formulation relying on an aqueous two-phase emulsion, which contains two immiscible aqueous phases of cell/GelMA mixture encapsulating droplets of poly(ethylene oxide) (PEO), is photocrosslinked following bioprinting to fabricate predesigned cell-laden hydrogel constructs at a reduced temperature for increased viscosity. Porous structure of the 3D bioprinted construct is formed by subsequently removing the PEO phase from the GelMA hydrogel during incubation in cell culture medium (Fig. 2B). The development of the aqueous two-phase emulsion bioinks enabled controllable pore size distribution through adjusting the volume ratio of the PEO/GelMA solutions, serving as a new strategy to engineer porous-structured tissue constructs using bioprinting (Fig. 2C). Cells within the 3D-bioprinted porous cell-laden hydrogel patterns showed enhanced cell viability, spreading, and proliferation compared to the standard (i.e., non-porous) GelMA constructs (Fig. 2D).

Alginate-templated GelMA bioink

Besides direct deposition, low-viscosity biomacromolecules such as GelMA at low concentrations can also be extrusion-bioprinted in a molecular-templated manner. For this, the alginate/GelMA composite bioink and the microfluidic bioprinting technology based on a coaxial needle have been developed, where the bioink is delivered from the core and the ionic crosslinking agent ($CaCl_2$ solution) is sheathed on the side (Fig. 3A) [32–35]. The introduction of alginate in the composite bioink enhances the viscosity of the GelMA solution. More importantly, the alginate component allows for rapid physical crosslinking by $CaCl_2$ during the bioprinting process to maintain the structural fidelity of the microfibrous constructs [36], followed by photocrosslinking of the GelMA component using UV illumination. This two-step crosslinking procedure enabled bioprinting of microfibrous structures based on GelMA/alginate (Fig. 3B-a, b) [35]. Interestingly, alginate could be removed following bioprinting, through chelation of Ca^{2+} by immersing the constructs in a solution of ethylenediaminetetraacetic acid (EDTA), to leave behind microfibers consisting of almost pure GelMA (Fig. 3B-c). As

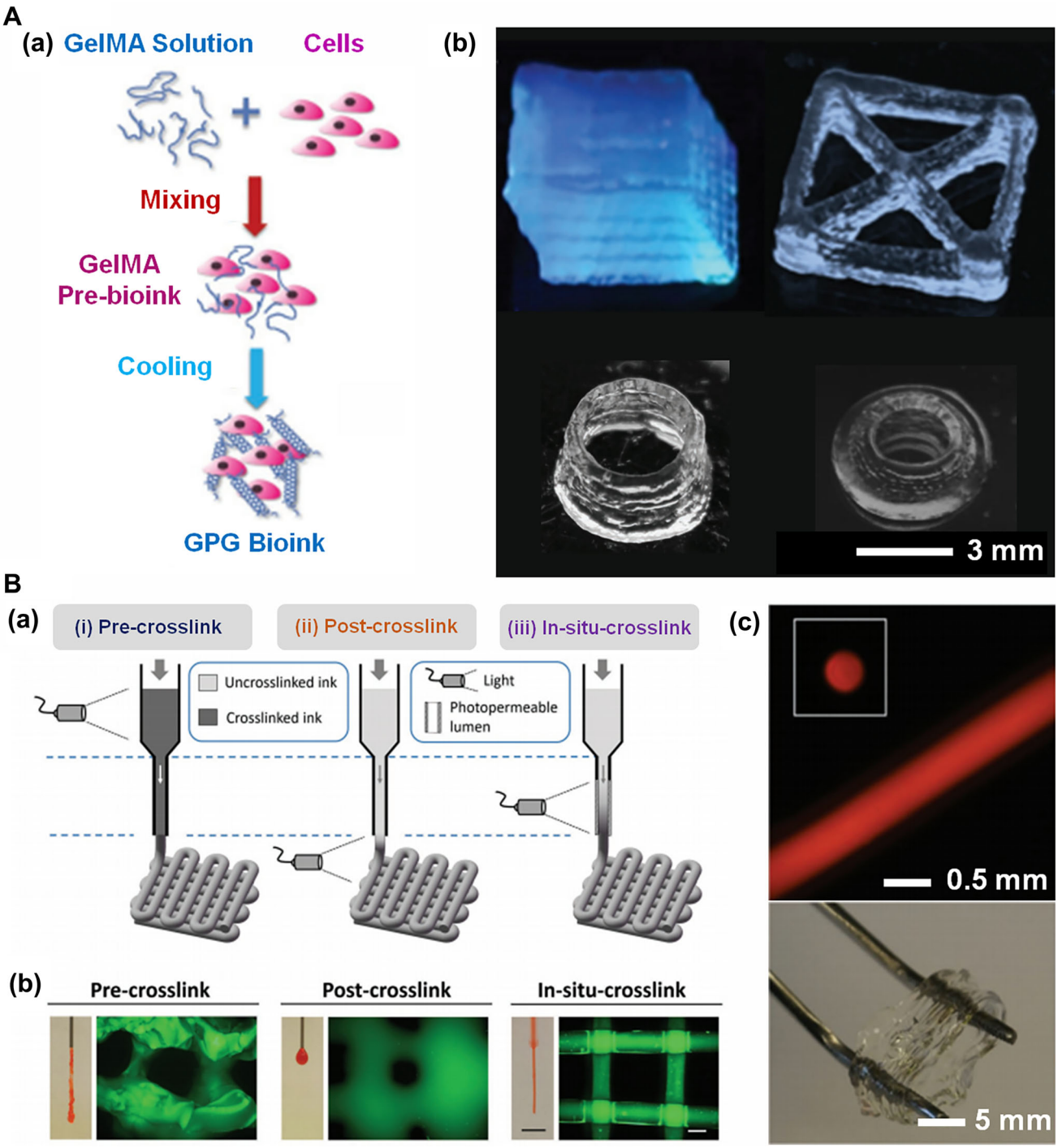

Fig. 1 Pure GelMA bioink. **A** Direct bioprinting of the pure GelMA bioink by a cooling process to form GPG prior to bioprinting. **a** Schematic of the bioink preparation. **b** Photographs showing the bioprinted structures (4 w/v% GelMA in GPG). Reproduced with permission [15]. **B** Direct bioprinting of the pure GelMA bioink through in situ photocrosslinking. **a** Schematic diagram of three photocrosslinking methods: before (pre-crosslink), after (post-crosslink), and during (in situ crosslink) extrusion. **b** Fluorescence images showing the resolution of the structures bioprinted by three different photocrosslinking methods. **c** Images showing the bioprinted filament and ring (5 w/v% GelMA). Reproduced with permission [30]

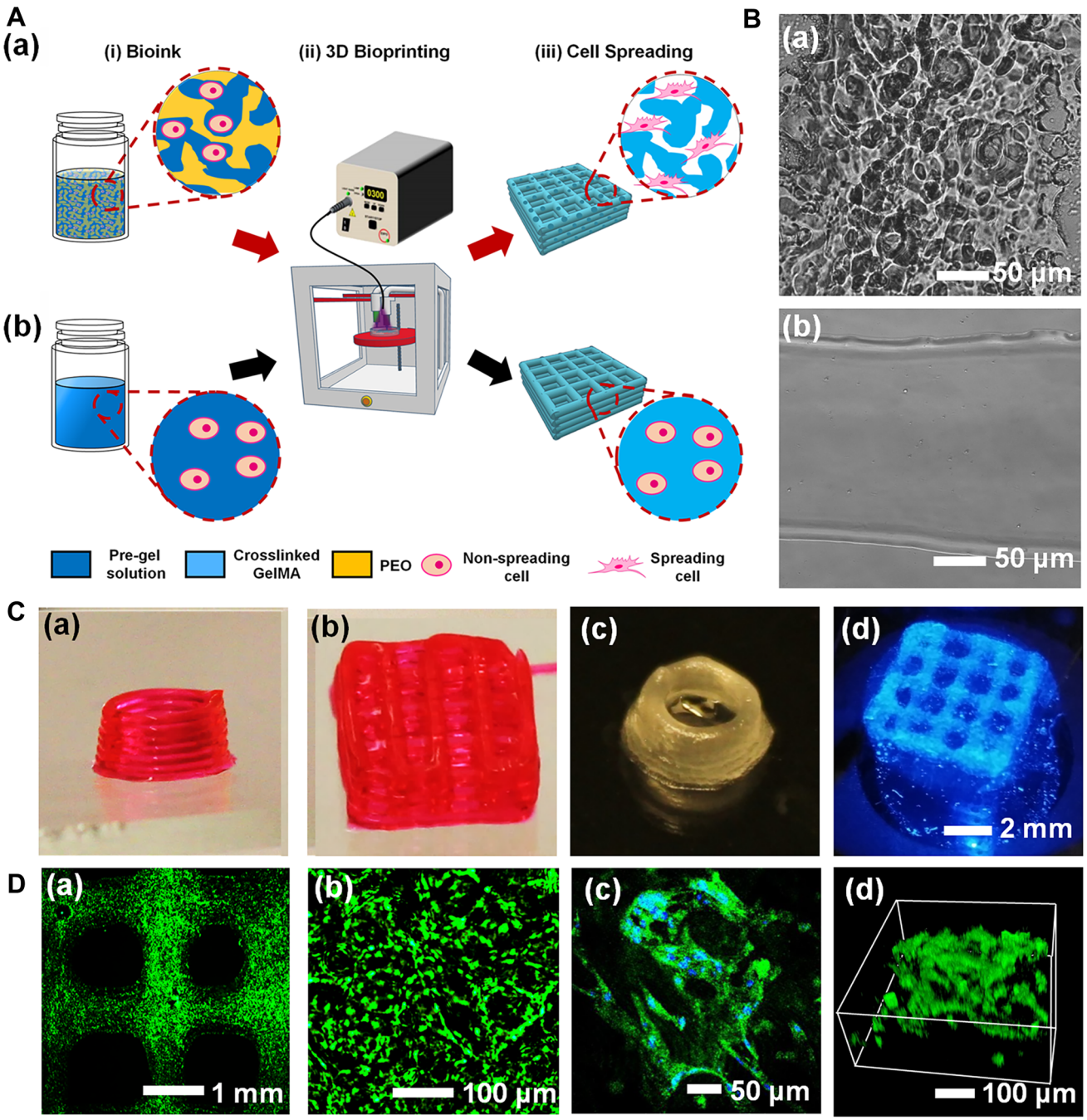

Fig. 2 Pore-forming GelMA bioink. **A** Schematics of 3D bioprinting of **a** a porous hydrogel structure using the pore-forming GelMA bioink and **b** a conventional hydrogel structure using the pure GelMA bioink. **B** Images showing the interior structure of patterns bioprinted with **a** pore-forming GelMA bioink and **b** pure GelMA bioink. **C** Photographs of 3D bioprinted multilayered GelMA hydrogel patterns with **a**, **b** pure GelMA bioink and **c**, **d** pore-forming GelMA bioink. **D** Fluorescence images of NIH/3T3 fibroblasts in GelMA hydrogel patterns bioprinted with pore-forming GelMA bioink. **c**, **d** Cell spreading within GelMA hydrogel constructs bioprinted with pore-forming GelMA bioink. Reproduced with permission [31]

such, microfibers at lower concentrations of GelMA could be bioprinted, leading to improved cell spreading, migration, and proliferation (Fig. 3C) [33].

Strategies for bioprinting GelMA-based bioinks

Several bioprinting techniques based on modifications of extrusion bioprinting, including sacrificial bioprinting and

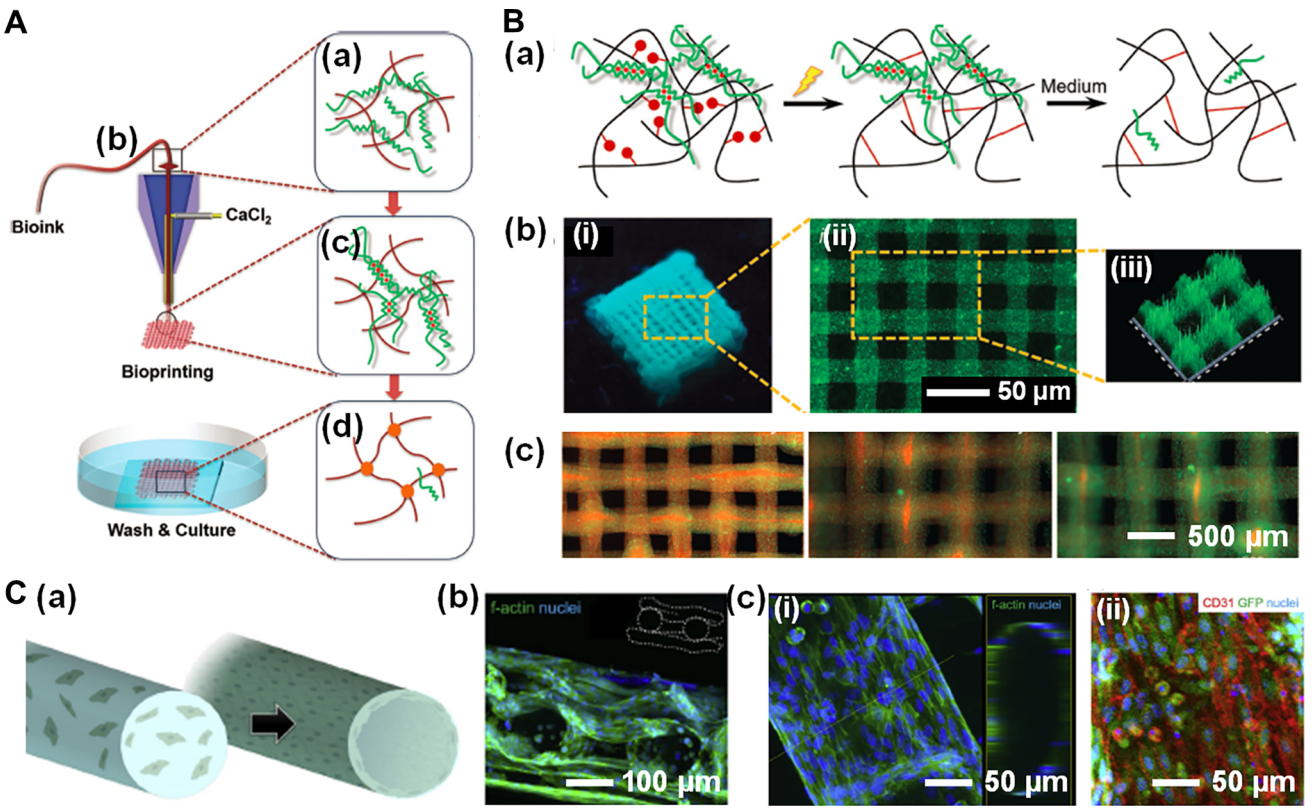

Fig. 3 Alginate-templated GelMA bioink. **A** Schematics of the bioprinting process: **a** preparation of templated GelMA bioink containing alginate and GelMA; **b** construction of a core–sheath coaxial nozzle, where the alginate-templated GelMA bioink is delivered through the core flow and the $CaCl_2$ solution is co-delivered through the sheath flow; **c** ionic crosslinking of the alginate component by Ca^{2+}; and **d** formation of the GelMA hydrogel through a secondary photocrosslinking, followed by gradual removal of alginate using a bath of Ca^{2+} chelator. **B** Bioprinting of microfibrous structures based on alginate-templated GelMA bioink. **a** Schematics showing two-step crosslinking procedure and subsequent removal of alginate. **b i** Photograph and **ii**, **iii** fluorescence micrographs showing a bioprinted multilayered construct; **c** Fluorescence microscopic images showing the release of alginate. Reproduced with permission [35]. **C a** Schematic representation showing the encapsulated HUVECs spreading in the bioprinted microfibers. **b** and **c** Confocal fluorescence micrographs showing the spreading of HUVECs in the bioprinted microfibrous structures using alginate-templated GelMA bioink following removal of the alginate component. Reproduced with permission [33]

hollow tube bioprinting, have been developed in addition to direct extrusion bioprinting to generate GelMA-based tissue constructs. Besides, GelMA-based bioinks can also be applied to non-extrusion bioprinting strategies for tissue fabrication.

Sacrificial bioprinting

Sacrificial bioprinting has been developed to produce hydrogel constructs containing interconnected vessel-like structures (Fig. 4A-a, b) [37]. As a sacrificial material, Pluronic F-127 microfibers are first bioprinted as the templates in arbitrary shapes, where GelMA pre-polymer bioink is subsequently filled in the surrounding space and photocrosslinked. The GelMA block with embedded microchannels can be obtained by removal of the Pluronic templates through immersing the construct at a low temperature (<4 °C) to liquefy the material and flushing it away. Endothelial cells could be finally seeded into the hollow microchannels to form biologically relevant blood vessels (Fig. 4A-c).

Alternatively, the sacrificial templates may also be physically extracted. For example, using agarose as the bioink, which forms a mechanically robust solid hydrogel at room temperature or lower, microfibers could be bioprinted and GelMA constructs containing hollow microchannels could be fabricated in a similar manner (Fig. 4B-a, b) [38–40]. Again, these hollow microchannels may be further populated with a monolayer of endothelial cells (Fig. 4B-c), and the formed endothelium was functional serving as an efficient barrier deferring the diffusion of biomolecules into the surrounding GelMA matrix (Fig. 4B-d) [39].

Hollow tube bioprinting

The bioprinted microfibrous structures composed of solid interiors, as shown in Fig. 3C, were not perfusable. To mimic

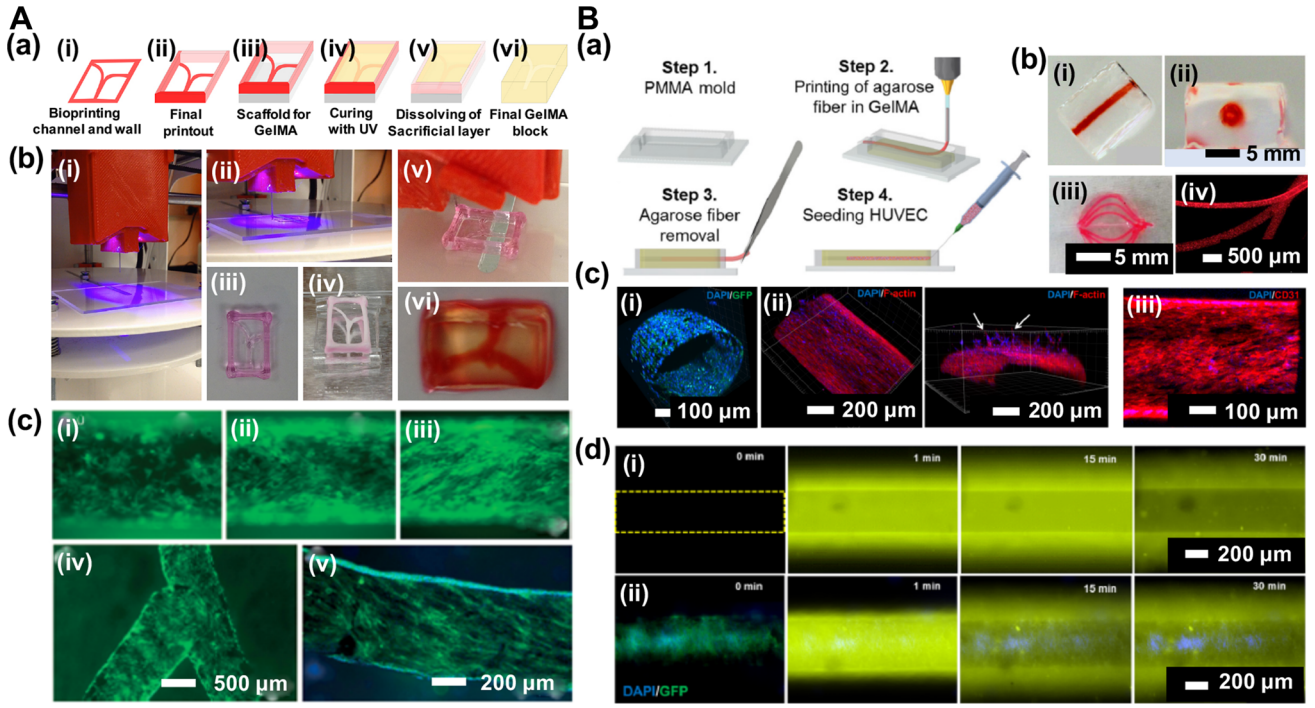

Fig. 4 Sacrificial bioprinting. **A a** Schematic of the sacrificial bioprinting process using Pluronic F-127 as a sacrificial material. **b** Photographs showing the bioprinting procedure and fabricated hydrogel construct with a central hollow microchannel structure. **c** Endothelialization of the hollow microchannel inside the GelMA construct for **c-i** 0 day, **c-ii** 1 day, and **c-iii** 2 days in a linear microchannel, and **c-iv** in a branching microchannel, where HUVECs were labeled with green fluorescent protein (GFP); **c-v** CD31 staining of the HUVECs. Reproduced with permission [37]. **B a** Schematic of the sacrificial bioprinting process using agarose as a sacrificial template and **b** photographs showing a linear microchannel and a branching microchannel embedded inside the GelMA matrix. **c** Formation of endothelial monolayer in the microchannel of the GelMA construct and its outward sprouting. **d** Diffusion profiles of rhodamine 6G into the microchannel **d-i** without and **d-ii** with the endothelium at different time points. Reproduced with permission [39]

cannular tissues widely present throughout the human body, another technique based on microfluidic bioprinting has been developed to directly bioprint perfusable hollow microfibers [41–43]. In a typical setup, a multilayered concentric nozzle is utilized, where the composite bioink containing alginate, GelMA, and other structural molecules is delivered from the middle layer, and the crosslinking agent $CaCl_2$ solution is flown from both interior and exterior, leading to the generation of a tubular structure in a single extrusion process (Fig. 5A-a) [10]. Volumetric structures consisting of a single hollow tube could be bioprinted (Fig. 5A-b), which was demonstrated to be perfusable across the entire layers (Fig. 5A-c-i). Vascular cells could be further encapsulated into the bioink during extrusion, forming the biologically relevant hollow vessel structure following a period of culture (Fig. 5A-c-ii). With the inclusion of more layers in the concentric nozzle setup, tunable numbers of walls in a hollow fiber (e.g., between single and double layers at regular intervals) could be achieved by switching the bioink delivery in the different layers on or off at desired time points (Fig. 5B) [44].

Contrarily, the hollow alginate microfibers may as well serve as structural supports for building cell-laden constructs in low-stiffness GelMA hydrogels, providing cells with soft microenvironments suitable for engineering certain tissue types [45]. Different with the hollow GelMA-based microfibers discussed above, here a mixture of GelMA and $CaCl_2$ solution is employed as the core while the alginate solution is extruded from the sheath (Fig. 5C-a), resulting in bioprinted 3D microfibrous constructs where the GelMA bioink is embedded within the microfibers and subjected to subsequent photocrosslinking. The encapsulated cells showed differential morphologies when the GelMA bioinks used in the cores of the microfibers had different concentrations (Fig. 5C-b). The concentration (down to 1 w/v%) of GelMA that could be bioprinted using this strategy was even lower than that possible through direct extrusion bioprinting with the GPGs [15].

Non-extrusion-based bioprinting

The above-mentioned bioprinting strategies relying on direct or indirect extrusion are easy to realize, but the processes are generally slow. In comparison, a few non-extrusion-based bioprinting strategies could shorten the time needed for tissue

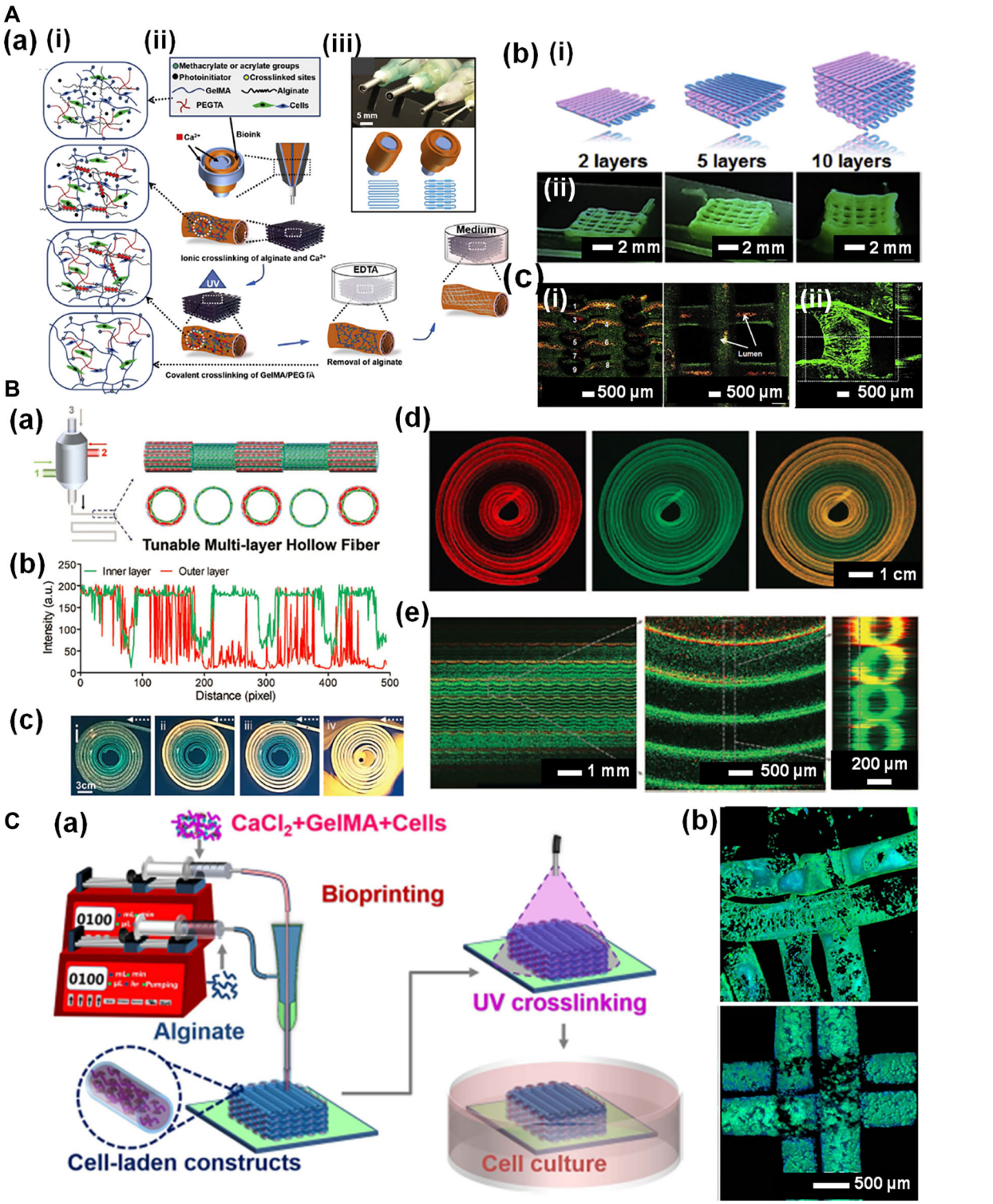

Fig. 5 Hollow fiber bioprinting. **A a** Schematic diagram showing direct bioprinting of perfusable hollow microfibers. **b** Bioprinted tubular constructs with different numbers of layers. **c-i** Perfusion of bioprinted hollow fibers. **c-ii** Vascular cells in bioprinted hollow fibers. Reproduced with permission [10]. **B a** Schematic illustration of controllable tuning of layers of a bioprinted hollow fiber. **b** Intensity of green and red signals at regions of single and double layers of a bioprinted hollow tube containing green fluorescence in the inner layer and red fluorescence in the outer layer. **c** Perfusion of the bioprinted continuous hollow fiber with different layers of walls. **d** Fluorescence microscopy images of a bioprinted hollow tube containing transitions from double to single to double layers. **e** Dynamic conversion from double-layered to single-layered hollow fiber in a single bioprinting process. Reproduced with permission [44]. **C a** Schematic diagram showing the strategy of alginate hollow microfiber-templated GelMA bioprinting. **b** Spreading of MDA-MB-231 breast cancer cells in 1.0 w/v% and 2.0 w/v% GelMA hydrogels within the bioprinted alginate hollow microfibers. Reproduced with permission [45]

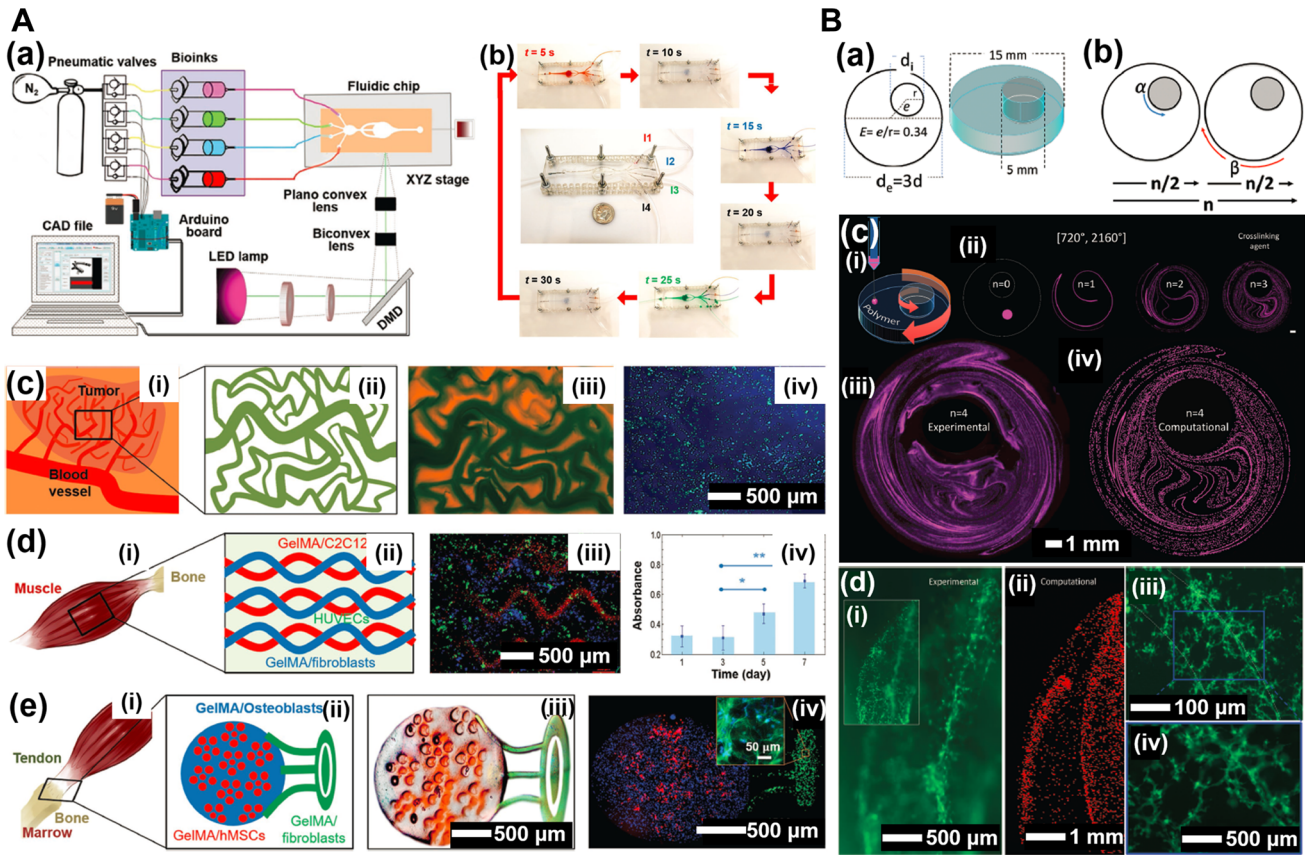

Fig. 6 Non-extrusion-based bioprinting. **A** DMD bioprinting. **a** Schematic of the DMD bioprinter setup, including a UV lamp, optical lenses and objectives, a DMD chip, and a microfluidic chip device. **b** The microfluidic device for different bioink injections. **c**–**e** A set of GelMA-encapsulated complex tissue constructs: **c** a vascularized tumor, **d** a muscle strip, and **e** a musculoskeletal interface. Reproduced with permission [48]. **B** Chaotic bioprinting. **a** Schematic and **b** mechanism of the chaotic bioprinter setup (Joule bearing flow system). The cells are encapsulated within GelMA hydrogel by rotating two eccentrically located cylinders in pre-programmed directions and angles, followed by photocrosslinking. **c** Characterization of produced chaotic structure (fluorescent dye within the GelMA hydrogel). **d** Chaotic-bioprinted cells within GelMA hydrogel. Cells were spreading along a string produced by chaotic bioprinting. Reproduced with permission [49]

fabrication and possibly enhance the resolution of features in the generated tissue constructs.

The digital micromirror device (DMD), an integrated microelectromechanical system containing controllable arrays of micromirrors at a high number, provides a high-speed platform for bioprinting [46]. The DMD bioprinting is operated by projecting a pattern of light onto the bottom layer of the bioink (such as GelMA) hosted in a reservoir [47]. Through exposure, each photosensitive bioink layer is photocrosslinked, which, followed by vertical movement of the substrate to expose a new layer of the bioink, allows for the generation of a 3D pattern when this pair of operations is repeated. Recently, a DMD bioprinting technology integrated with a microfluidic chip serving as the reservoir enabling sequential injection of different bioinks was developed to bioprint multicomponent tissue constructs (Fig. 6A-a, b) [48]. A set of complex tissue constructs with well-defined structures based on GelMA encapsulating various cell types was bioprinted, including a vascularized tumor (Fig. 6A-c), a muscle strip (Fig. 6A-d), and a musculoskeletal interface (Fig. 6A-e). The cells were found to be viable and proliferating within the bioprinted multicomponent GelMA constructs.

More recently and interestingly, an unconventional chaotic bioprinting technique was reported to control the precise positioning of microscale and nanoscale features in the bioprinted structures [49]. The chaotic bioprinting is designed to create fine architectures by flow itself in a controllable and reproducible manner in a solid matrix, where the bioink and the matrix can be either the same material or different materials. For this, a customized Joule bearing device, which contained an outer cylinder and an inner cylinder, was constructed (Fig. 6B-a). By rotating the cylinders in opposite directions with a defined angle, the bioink droplet in the matrix could be elongated forming a pattern that was highly predictable as a function of the rotation and material parameters (Fig. 6B-b, c). As an example, cells could be embedded in the GelMA bioink droplet, in which after rotation (bioprinting) high-resolution patterns of cells in the

surround GelMA matrix could be generated to mimic, for example, multiscale vascularization, revealing also favorable cell spreading (Fig. 6B-d).

Conclusion and future perspective

To date, various types of GelMA-based bioinks have been developed, allowing us to bioprint complex tissue constructs that were difficult to produce in the past. On the other hand, improved bioprinting strategies have further enabled us to fabricate complex tissue-like structures using different GelMA-based bioinks. We envision that GelMA as a cost-effective yet biocompatible and bioactive material will play an important role in bioprinting to facilitate the generation of functional tissues and biomimetic tissue models for widespread applications in tissue engineering, regenerative medicine, pharmaceutics, and precision medicine among others.

Acknowledgements The authors gratefully acknowledge funding from the National Institutes of Health (K99CA201603, R21EB025270, R21EB026175) and Doctoral New Investigator Grant from American Chemical Society Petroleum Research Fund (56840-DNI7). G. L. Y. acknowledges Natural and Science Foundation of Hubei Province (2014CFB778).

Compliance with ethical standards

Conflict of interest The authors declare no conflict of interests.

References

1. Griffith LG, Naughton G (2002) Tissue engineering–current challenges and expanding opportunities. Science 295:1009–1014
2. Atala A (2009) Engineering organs. Curr Opin Biotech 20:575–592
3. Lanza R, Langer R, Vacanti JP (2011) Principles of tissue engineering. Academic press, Cambridge
4. Langer R (2007) Tissue engineering: perspectives, challenges, and future directions. Tissue Eng 13:1–2
5. Khademhosseini A, Langer R (2016) A decade of progress in tissue engineering. Nat Protoc 11:1775
6. Chaudhari AA, Vig K, Baganizi DR, Sahu R, Dixit S, Dennis V, Singh SR, Pillai SR (1974) Future prospects for scaffolding methods and biomaterials in skin tissue engineering: a review. Int J Mol Sci 2016:17
7. Makris EA, Gomoll AH, Malizos KN, Hu JC, Athanasiou KA (2015) Repair and tissue engineering techniques for articular cartilage. Nat Protoc 11:21
8. Zhang YS, Yue K, Aleman J, Mollazadeh-Moghaddam K, Bakht SM, Yang J, Jia W, Dell'Erba V, Assawes P, Shin SR (2017) 3D bioprinting for tissue and organ fabrication. Ann Biomed Eng 45:148–163
9. Murphy SV, Atala A (2014) 3D bioprinting of tissues and organs. Nat Biotechnol 32:773
10. Jia W, Gungor-Ozkerim PS, Zhang YS, Yue K, Zhu K, Liu W, Pi Q, Byambaa B, Dokmeci MR, Shin SR (2016) Direct 3D bioprinting of perfusable vascular constructs using a blend bioink. Biomaterials 106:58–68
11. Liu W, Zhang YS, Heinrich MA, De Ferrari F, Jang HL, Bakht SM, Alvarez MM, Yang J, Li YC, Trujillo-de Santiago G (2017) Rapid continuous multimaterial extrusion bioprinting. Adv Mater 29:1604630
12. Ozbolat IT, Hospodiuk M (2016) Current advances and future perspectives in extrusion-based bioprinting. Biomaterials 76:321–343
13. Kang H-W, Lee SJ, Ko IK, Kengla C, Yoo JJ, Atala A (2016) A 3D bioprinting system to produce human-scale tissue constructs with structural integrity. Nat Biotechnol 34:312
14. Hölzl K, Lin S, Tytgat L, Van Vlierberghe S, Gu L, Ovsianikov A (2016) Bioink properties before, during and after 3D bioprinting. Biofabrication 8:032002
15. Liu W, Heinrich MA, Zhou Y, Akpek A, Hu N, Liu X, Guan X, Zhong Z, Jin X, Khademhosseini A (2017) Extrusion bioprinting of shear-thinning gelatin methacryloyl bioinks. Adv Healthc Mater 6:1601451
16. Wang Z, Kumar H, Tian Z, Jin X, Holzman JF, Menard F, Kim K (2018) Visible light photoinitiation of cell-adhesive gelatin methacryloyl hydrogels for stereolithography 3D bioprinting. ACS Appl Mater Interfaces 10:26859–26869
17. Klotz BJ, Gawlitta D, Rosenberg AJ, Malda J, Melchels FP (2016) Gelatin-methacryloyl hydrogels: towards biofabrication-based tissue repair. Trends Biotechnol 34:394–407
18. Wu D, Yu Y, Tan J, Huang L, Luo B, Lu L, Zhou C (2018) 3D bioprinting of gellan gum and poly (ethylene glycol) diacrylate based hydrogels to produce human-scale constructs with high-fidelity. Mater Des
19. Huang Y, Zhang XF, Gao G, Yonezawa T, Cui X (2017) 3D bioprinting and the current applications in tissue engineering. Biotechnol J 12:1600734
20. Axpe E, Oyen ML (1976) Applications of alginate-based bioinks in 3D bioprinting. Int J Mol Sci 2016:17
21. Luo Y, Luo G, Gelinsky M, Huang P, Ruan C (2017) 3D bioprinting scaffold using alginate/polyvinyl alcohol bioinks. Mater Lett 189:295–298
22. Daly AC, Critchley SE, Rencsok EM, Kelly DJ (2016) A comparison of different bioinks for 3D bioprinting of fibrocartilage and hyaline cartilage. Biofabrication 8:045002
23. Lee H, Cho D-W (2016) One-step fabrication of an organ-on-a-chip with spatial heterogeneity using a 3D bioprinting technology. Lab Chip 16:2618–2625
24. Jungst T, Smolan W, Schacht K, Scheibel T, Groll J (2015) Strategies and molecular design criteria for 3D printable hydrogels. Chem Rev 116:1496–1539
25. Yue K, Trujillo-de Santiago G, Alvarez MM, Tamayol A, Annabi N, Khademhosseini A (2015) Synthesis, properties, and biomedical applications of gelatin methacryloyl (GelMA) hydrogels. Biomaterials 73:254–271
26. Yin J, Yan M, Wang Y, Fu J, Suo H (2018) 3D bioprinting of low-concentration cell-laden gelatin methacrylate (GelMA) bioinks with a two-step cross-linking strategy. ACS Appl Mater Interfaces 10:6849–6857
27. Billiet T, Gevaert E, De Schryver T, Cornelissen M, Dubruel P (2014) The 3D printing of gelatin methacrylamide cell-laden tissue-engineered constructs with high cell viability. Biomaterials 35:49–62
28. Bertassoni LE, Cardoso JC, Manoharan V, Cristino AL, Bhise NS, Araujo WA, Zorlutuna P, Vrana NE, Ghaemmaghami AM, Dokmeci MR (2014) Direct-write bioprinting of cell-laden methacrylated gelatin hydrogels. Biofabrication 6:024105
29. Schuurman W, Levett PA, Pot MW, van Weeren PR, Dhert WJA, Hutmacher DW, Melchels FPW, Klein TJ, Malda J (2013) Gelatin-methacrylamide hydrogels as potential biomaterials for

fabrication of tissue-engineered cartilage constructs. Macromol Biosci 13:551–561
30. Ouyang L, Highley CB, Sun W, Burdick JA (2017) A generalizable strategy for the 3D bioprinting of hydrogels from nonviscous photo-crosslinkable inks. Adv Mater 29:1604983
31. Ying G-L, Jiang N, Maharjan S, Yin Y-X, Chai R-R, Cao X, Yang J-Z, Miri AK, Hassan S, Zhang YS (2018) Aqueous two-phase emulsion bioink-enabled 3D bioprinting of porous hydrogels. Adv Mater. https://doi.org/10.1002/adma.201805460
32. Colosi C, Shin SR, Manoharan V, Massa S, Constantini M, Barbetta A, Dokmeci MR, Dentini M, Khademhosseini A (2015) Microfluidic bioprinting of heterogeneous 3D tissue constructs using low viscosity bioink. Adv Mater 28:677–684
33. Zhang YS, Arneri A, Bersini S, Shin S-R, Zhu K, Malekabadi ZG, Aleman J, Colosi C, Busignani F, Dell'Erba V, Bishop C, Shupe T, Demarchi D, Moretti M, Rasponi M, Dokmeci MR, Atala A, Khademhosseini A (2016) Bioprinting 3D microfibrous scaffolds for engineering endothelialized myocardium and heart-on-a-chip. Biomaterials 110:45–59
34. Zhang YS, Pi Q, van Genderen AM (2017) Microfluidic bioprinting for engineering vascularized tissues and organoids. J Vis Exp 126:e55957
35. Zhu K, Chen N, Liu X, Mu X, Zhang W, Wang C, Zhang YS (2018) A general strategy for extrusion bioprinting of bio-macromolecular bioinks through alginate-templated dual-stage crosslinking. Macromol Biosci 18:1800127
36. Yetisen AK, Jiang N, Fallahi A, Montelongo Y, Ruiz-Esparza GU, Tamayol A, Zhang YS, Mahmood I, Yang SA, Kim KS (2017) Glucose-sensitive hydrogel optical fibers functionalized with phenylboronic acid. Adv Mater 29:1606380
37. Zhang YS, Davoudi F, Walch P, Manbachi A, Luo X, Dell'Erba V, Miri AK, Albadawi H, Arneri A, Li X, Wang X, Dokmeci MR, Khademhosseini A, Oklu R (2016) Bioprinted thrombosis-on-a-chip. Lab Chip 16:4097–4105
38. Bertassoni LE, Cecconi M, Manoharan V, Nikkhah M, Hjortnaes J, Cristino AL, Barabaschi G, Demarchi D, Dokmeci MR, Yang Y, Khademhosseini A (2014) Hydrogel bioprinted microchannel networks for vascularization of tissue engineering constructs. Lab Chip 14:2202–2211
39. Massa S, Seo J, Arneri A, Bersini S, Cha B-H, Antona S, Enrico A, Gao Y, Hassan S, Cox JPA, Zhang YS, Dokmeci MR, Khademhosseini A, Shin S-R (2017) Bioprinted 3D vascularized tissue model for drug toxicity analysis. Biomicrofluidics 11:044109
40. Zhang YS, Duchamp M, Ellisen LW, Moses MA, Khademhosseini A (2017) Recapitulating mammary ductal carcinoma microenvironment in vitro using sacrificial bioprinting. In: AACR 2017, Washington DC
41. Yu Y, Zhang Y, Martin JA, Ozbolat IT (2013) Evaluation of cell viability and functionality in vessel-like bioprintable cell-laden tubular channels. J Biomech Eng 135:091011–091011
42. Zhang Y, Yu Y, Ozbolat IT (2013) Direct bioprinting of vessel-like tubular microfluidic channels. J Nanotechnol Eng Med 4:020902
43. Zhang Y, Yu Y, Akkouch A, Dababneh A, Dolati F, Ozbolat IT (2015) In vitro study of directly bioprinted perfusable vasculature conduits. Biomater Sci 3:134–143
44. Pi Q, Maharjan S, Yan X, Liu X, Singh B, Van Genderen AM, Robledo-Padilla F, Parra-Saldivar R, Hu N, Jia W, Xu C, Kang J, Hassan S, Cheng H, Hou X, Khademhosseini A, Zhang YS (2018) Digitally tunable microfluidic bioprinting of multilayered cannular tissues. Adv Mater 30:1706913
45. Liu W, Zhong Z, Hu N, Zhou Y, Maggio L, Miri AK, Fragasso A, Jin X, Khademhosseini A, Zhang YS (2018) Coaxial extrusion bioprinting of 3D microfibrous constructs with cell-favorable gelatin methacryloyl microenvironments. Biofabrication 10:024102
46. Ma X, Qu X, Zhu W, Li Y-S, Yuan S, Zhang H, Liu J, Wang P, Lai CSE, Zanella F (2016) Deterministically patterned biomimetic human iPSC-derived hepatic model via rapid 3D bioprinting. Proc Natl Acad Sci 113:2206–2211
47. Han L-H, Mapili G, Chen S, Roy K (2008) Projection microfabrication of three-dimensional scaffolds for tissue engineering. J Manuf Sci Eng 130:021005
48. Miri AK, Nieto D, Iglesias L, Goodarzi Hosseinabadi H, Maharjan S, Ruiz-Esparza GU, Khoshakhlagh P, Manbachi A, Dokmeci MR, Chen S, Shin SR, Zhang YS, Khademhosseini A (2018) Microfluidics-enabled multimaterial maskless stereolithographic bioprinting. Adv Mater 30:1800242
49. Trujillo-de Santiago G, Alvarez MM, Samandari M, Prakash G, Chandrabhatla G, Rellstab-Sánchez PI, Byambaa B, Pour Shahid Saeed Abadi P, Mandla S, Avery RK, Vallejo-Arroyo A, Nasajpour A, Annabi N, Zhang YS, Khademhosseini A (2018) Chaotic printing: using chaos to fabricate densely packed micro- and nanostructures at high resolution and speed. Mater Horizons 5:813–822